View metadata, citation and similar papers at core.ac.uk

brought to you by CORE

provided by Queensland University of Technology ePrints Archive

Queensland University of Technology
Brisbane Australia

This is the author's version of a work that was submitted/accepted for publication in the following source:

AL-Dulaimi, Khamael, Tomeo-Reyes, Inmaculada, Banks, Jasmine, & Chandran, Vinod
(2016)
White blood cell nuclei segmentation using level set methods and geometric active contours. In
*2016 International Conference on Digital Image Computing: Techniques and Applications (DICTA)*, IEEE, Gold Coast, QLD, pp. 1-7.

This file was downloaded from: https://eprints.qut.edu.au/103066/

**© 2016 IEEE**

Personal use of this material is permitted. Permission from IEEE must be obtained for all other uses, in any current or future media, including reprinting/republishing this material for advertising or promotional purposes, creating new collective works, for resale or redistribution to servers or lists, or reuse of any copyrighted component of this work in other works.

**Notice**: *Changes introduced as a result of publishing processes such as copy-editing and formatting may not be reflected in this document. For a definitive version of this work, please refer to the published source:*

*https://doi.org/10.1109/DICTA.2016.7797097*

# White Blood Cell Nuclei Segmentation Using Level Set Methods and Geometric Active Contours

Khamael AL-Dulaimi, Inmaculada Tomeo-Reyes, Jasmine Banks, Vinod Chandran

School of Electrical Engineering and Computer Science, Queensland University of Technology
Brisbane, QLD, Australia

khamaelabbaskhudhair.aldulaimi@hdr.qut.edu.au, {inma.tomeoreyes, j.banks, v.chandran}@qut.edu.au

***Abstract*— A new method for segmenting white blood cells nuclei in microscopic images is presented. Challenges to accurate segmentation include intra-class variation of the nuclei cell boundaries, non-uniform illumination, and changes in the cell topology due to its orientation and stage of maturity. In this research, level set methods and geometric active contours are used to segment the nucleus of white blood cells from the cytoplasm and the cell wall. Level set methods use morphological operations to estimate an initial cell boundary and are fully automated. Geometric active contours are less computationally complex and adapt better to the curve topology of the cell boundary than parametric active contours, which have been previously used for white blood cell segmentation. Segmentation performance is compared with other segmentation methods using the Berkeley benchmark database and the proposed method is shown to be superior using various indices.***

***Keywords—geometric active contours; parametric active contours; level set methods; white blood cell segmentation.***

## I. INTRODUCTION

White blood cell (WBC) segmentation is an important technology in medical imaging. In the field of cancer diagnosis, automatic segmentation of WBCs is an important step in the process of counting, locating, and identifying different types of cells. There are three types of WBC: Granulocytes, Monocytes and Lymphocytes. They are further classified into seven sub-types. *Granulocytes* can be Band neutrophils, Basophils or Eosinophils. *Monocytes* can be Macrophages or Dendritic cells, and *Lymphocytes* can be B-lymphocytes or T-lymphocytes. Each WBC structure contains a cell wall, a nucleus and cytoplasm [1] as shown in Fig.1.

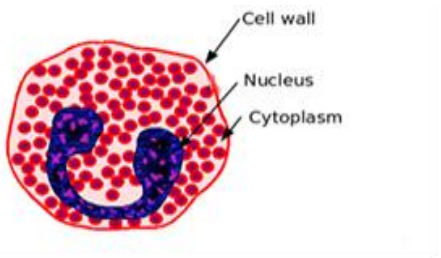


Fig. 1. Diagram of WBC (Eosinophil cell).

The input images of WBCs used in this work are taken from peripheral blood smear samples on microscope slides [2][3]. These images are obtained by placing the slides under a compound or optical microscope with certain light and magnification and recording them with a digital camera. Microscopic images of the cells are obtained after a staining process which results in different coloration of the cells nuclei and cytoplasm and the blood image background (plasma). There are many types of stains (e.g. Giemsa stain, Wright stain, Wright-Giemsa stain and Leishman stain), but most of them dye the nucleus dark purple or pink [4]. The stains may also show up the granules present in the cytoplasm of some WBCs. While each cell has a darkly stained nucleus, the cytoplasm may not be consistently prominent in all cells. The staining process yields sufficient contrast for segmentation and classification of individual cells. The accuracy of the procedure depends on the algorithms used and their ability to extract useful information while being robust to variations.

The most useful shape information for cell classification comes from the nuclei of the cells. Nuclei have different shapes and sizes and might present one or more lobes. Accurate segmentation of the nuclei is therefore a critical step in the segmentation process. *Granulocytes* have large elongated or lobed nuclei. Neutrophils have multi-lobed nuclei (3-4 lobes normally). Basophils show large and very numerous granules which often mask the nucleus [5]. Eosinophils often have two-lobed nuclei connected by a band of nuclear material. *Monocytes* contain just one nucleus which is rarely or barely lobed. The nucleus in monocytes is often bend-shaped (horseshoe) or reniform (kidney-shaped). Macrophages have a large-size single nucleus that is often kidney-shaped [6]. Dendritic cells have a small and round-shaped nucleus, which, as the cell matures, turns into a large nucleus with an irregular star shape and cytoplasmic protrusions (dendrites) [7]. *Lymphocytes* can have a small or large nucleus depending on the maturation stage, and the nucleus is usually round or slightly oval. More specifically, B-cells have oval nuclei, while T-cells have circular nuclei. Fig. 2 shows an original WBC image that contains six WBC sub-types. The shape of the nucleus can be clearly seen in each case.

Ministry of Higher Education and Scientific Research (Iraq)

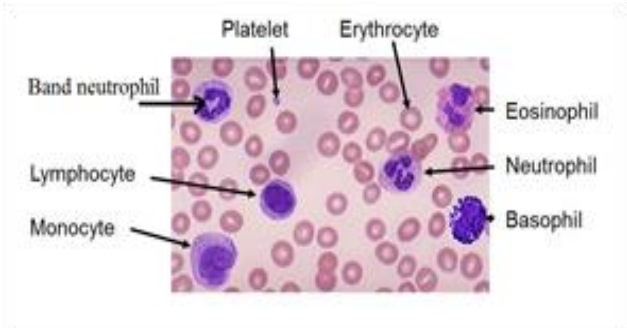


Fig. 2. Colour image of WBCs (24 bits per pixel and size 331×504).

Changes in the shape, area, eccentricity, compactness, colour or position of WBC nuclei can indicate that the human body may be affected by a disease such as leukaemia, some immunological disorders, and certain types of cancer [1]. Therefore, WBC analysis is a useful diagnostic tool. Automated and reliable WBC segmentation and classification can reduce the cost of this process and make it faster [5].

## II. Related Work

Many methods have been proposed in the literature to segment WBCs. One of the earliest works on WBC segmentation was presented by Norgren *et al.* [8], who proposed an automatic method to analyse normal and abnormal WBCs in a blood smear. They used whole-field histogram and thresholding, together with a series of clean-up operations to perform segmentation. In [9], a method was proposed to separate WBCs from other components in blood images, such as the background, red blood cells and cytoplasm, by merging the Teager/Kaiser filter with morphological operations. Ellipse matching and B-spline snakes were used for segmentation of WBCs in [10]. Sarrafzadeh and Dehnavi [11] used region growing, edge detection, filtering, and mathematical morphology to determine the boundaries of blood cells, extract features, and separate red blood cells, WBCs and platelets. They used K-means clustering and region growing to segment the nucleus and cytoplasm regions of WBCs. This method is not able to segment the nuclei well when there is cell division and there are two or more convex portions in the boundary or weak concavities.

Nucleus segmentation is required for feature extraction and classification of cells. The additional challenges in segmenting the nucleus boundary compared to the cell boundary can be addressed to some extent with the proposed method. Despite previous work in this field, automatic WBC segmentation is still challenging, particularly in the presence of non-uniform illumination and cell distortion. Level set with Geometric Active Contours (GACs) can be useful for the WBC nuclei segmentation problem.

### A. Level Set Methods via PACs and GACs

Level set methods were proposed by Osher and Sethian [12]. By using a Partial Differential Equation (PDE), they can describe propagating fronts, and can robustly adapt to a change in the topology of an interface. Several techniques have been used with level set methods to detect the boundary of an object, such as snake and region-based methods, and the watershed algorithm [12]. Recently, level set methods have been used in many fields, such as image processing, computer graphics, optimization, computational fluid dynamics, and computational geometry [12].

Parametric active contours (PACs) have been extensively utilised in computer vision and computer graphics for segmenting, visualizing, tracking, and quantifying different anatomic structures such as the face, retinal arteries, kidney, heart, brain tumours and even cellular structures such as neurons and chromosomes [13]. Different modifications have been implemented to solve estimation problems of the different shapes.

Level set methods via PACs, including (i) edge-based and (ii) region-based, are represented explicitly as parameterised boundaries in a Lagrangian formulation [14]. They are used to solve problems of shape estimation by reducing energy functions that take a minimum value when contours are smooth and reside on the boundaries of an object [15]. Level set methods via PACs convert the problem of boundary detection into a process of minimising an energy function subject to specific constraints by using a dynamic equation which has internal and external forces. During deformation, the internal force keeps the contour smooth and continuous, while the external force drives the contour towards an object boundary [16]. On the other hand, GACs solve the problem of changes in curve topology by using curve evolution [17]. GACs are represented implicitly as level sets of a 2-D distance function evolving according to an Eulerian formulation. They are based on level set techniques implemented via the theory of curve evolution and they do not use control points to determine the boundaries [14][18], as shown in Fig.3. GACs have been used for edge detection and segmentation of different types of medical images, such as magnetic resonance imaging (MRI), ultrasound, and computed tomography (CT).

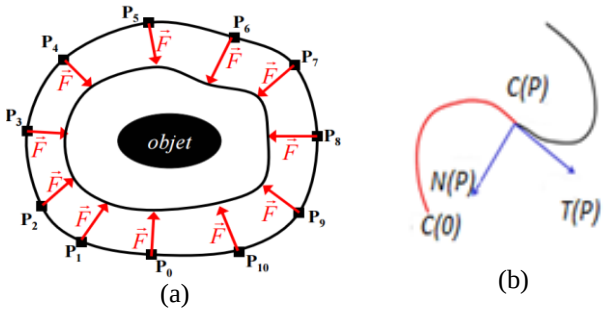


Fig. 3. PACs vs. GACs. a) PACs: $P_1$, $P_2$, etc. are control points and $F$ is the force [19]. b) GACs: $C$ is a curve and $C(0)$ (marked in red) is the zero level set or initial contour (arc length), $N(P)$ is the normal vector and $T(P)$ is the tangent [20].

### B. Application to WBC Segmentation

A few researchers have proposed techniques to segment WBCs using level set methods and active contours. Based on the concept of topological dependence, the advantages of level set methods and watershed approaches were combined in [21], where the merging of nucleus and cell segments was

prevented by dynamically evolving the watershed lines at each time step. This solved the over-segmentation problem of the watershed method, but there were still overlapped nuclei and cells in some cases. In [22], level set methods and the Canny edge detector were used to resolve ambiguous boundaries of WBCs. Initial boundaries of WBCs were first obtained using level set methods, and Canny edge detection was later used to detect the boundary of the cells. After that, the level set method was used again to segment the nucleus of the WBCs. PACs were used to obtain the edges and contours of the cells. This technique segmented simple boundaries of WBCs well, but complex and overlapped boundaries of WBCs still required improvement. The level set method via PACs was also used in [23] to detect and find cancer affected WBCs. The modified level set method and a piecewise smooth function were used to obtain the contour of the WBC cell. The energy function of this contour was represented as internal energy defined within the contour itself to maintain its smoothness. While the method worked for some cells, it was difficult to detect the nuclei, and small cells were not segmented.

### *C. Motivation and Contribution*

WBCs segmentation is still prone to error because of several challenges. Firstly, illumination is non-uniform because of the different colour distribution in the images. Secondly, the variation of complex cells and nuclei boundaries makes it difficult to obtain the edge information and locate the cells accurately. Also, the different background sizes, shapes, and positions of cells under the microscope make it difficult to separate the nucleus from the cytoplasm and adjacent erythrocytes. In these situations, it is a problem to segment the nucleus and the cytoplasm using an edge detection algorithm. Existing techniques that use level set methods to segment WBCs are based on PACs. When level set techniques are implemented via PACs, they may have to be reparameterised if control points are added or removed [24]. This is useful to handle changes in the topology of the cell, which can grow or shrink. In [25], the problem of segmenting WBCs using level set methods via PACs is reduced to finding the curve(s) surrounding the nuclei of the cells. Control points are used to detect the curves directly despite issues involved in updating the control points, including potentially splitting or merging contours when control points separate or merge. Level set methods implemented via GACs have advantages over PACs, including their simpler computation and the ability to better adapt to changes in curve topology or distortions [26]. This results in improved segmentation of WBCs. Level set methods via GACs have not been used in WBCs segmentation to date.

The main contribution of this paper is the application, for the first time, of level set methods via GACs to segment the WBC nucleus from the cell wall and cytoplasm. The advantage of using level set methods via GACs lies in the combination of the theory of curve evolution and geometric flows [27]. This model allows automatic topological changes when preformed using level set methods based on a numerical algorithm. Using level set methods with GACs allows us to calculate an implicit surface based on an externally generated velocity field, in which we determine the curvature of an interface, direction, and distance to the nearest point on the surface. Surface motion can also be determined on GACs to track the interface and the shape of nuclei of WBCs as shown in Fig.7(c).

## III. Proposed Method for WBC Segmentation

In this paper, morphological operations, such as opening and closing morphological reconstruction, are used to initiate the reconstruction of WBCs [28][30]. Next, the level set method via GACs is implemented. This method has the advantage that it can perform numerical computations that involve curves, shapes and surfaces based on a fixed Cartesian grid without having to parameterise them (Eulerian approach) [24]. It evolves an initial curve known as the zero level set to the boundaries of objects based on the image pixels *f(x, y)*. The zero level set is where the level set function has the value zero and is considered as the initial contour.

In the level set method, an interface $C$ is represented as a level set of a higher dimensional level set function $\phi$. The level set function is initialised as the signed distance function from $C$ to the rest of the pixels of the image at position $(x, y)$, according to the following equation [27]:

$$\phi(x,y) = \pm d((x,y),C) \tag{1}$$

where $d((x,y)$ is the signed distance from the pixel position $(x,y)$ to the interface $C$. The distance is indicated as positive if the pixel is inside $C$, and negative if the pixel is outside $C$. Interface $C$ is considered as the zero level set and is written as:

$$C = \{(x,y) \mid \phi(x,y) = 0\} \tag{2}$$

The evolution of the surface in time is caused by forces or flow normal to the surface with a known speed $F$, and can be calculated according to equation (3) [27]. The speed $F$ of a point on the surface normal to the surface is used to pull or push the contour.

$$\frac{\partial \phi(x,y,t)}{\partial t} + F|\nabla \phi| = 0 \tag{3}$$

The level set function is evolved using a 3rd order accurate essentially non-oscillatory scheme (ENO3) [12]. The calculation of the derivatives using the ENO3 scheme is based on the input data. This is done by first extrapolating the beginning and end points of the data, and then generating the divided difference tables. Before the calculation, the input image $f(x, y)$ and speed term $F$ need to be extended over a window by 3 pixels. Derivatives calculation (both + and −) is based on forward Euler time discretization of a Hamilton-Jacobi equation which can be written as [27][12]:

$$\frac{\phi^{n+1} - \phi^n}{\Delta t} + \hat{H}^n(\phi_x^-, \phi_x^+; \phi_y^-, \phi_y^+) = 0 \tag{4}$$

$\hat{H}_n(\phi_x^-, \phi_x^+; \phi_y^-, \phi_y^+)$ is a numerical approximation of $H(\phi_x, \phi_y)$, where $H$ is called the numerical Hamiltonian and is defined as $H(\nabla\phi) = F|\nabla\phi|$. $\Delta t$ is the Euler time step, which can be calculated according to the following equation [12]:

$$\Delta t \max\left\{\frac{H1}{\Delta x}+\frac{H2}{\Delta y}\right\} \le 1 \qquad (5)$$

where $\Delta x$ and $\Delta y$ are the resolutions of the grid in the $x$ and $y$ dimensions, and $H1$ and $H2$ are, respectively, the partial derivatives of $H$ that relate to $\phi_x$ and $\phi_y$.

A level set method via GACs based on motion by mean curvature is used in this paper. It is calculated from the following evolution equation [27]:

$$\frac{\partial \phi(x,y,t)}{\partial t} = (\alpha\kappa(\phi(x,y,t)) + \nu)\left|\nabla\phi(x,y,t)\right| \qquad (6)$$

where ν is a constant value which is selected so that the value of $(\alpha\kappa(\phi(x, y, t)) + \nu)$ is always positive. This constant behaves as a force that pushes the curve toward the cell boundary when the curvature becomes negative. Choosing ν as a positive value increases the propagation speed. Here, $\kappa$ indicates the mean curvature of the level set function, aimed at controlling the regularity of the contour as the internal force, and is given by equation (7). The value of $\alpha$ is between 0 and 1, so that the balance between the robustness and regularity of the contour evolution can be controlled.

$$\kappa(\phi(x,y,t)) = div\left(\nabla\phi/\left\|\nabla\phi\right\|\right) \qquad (7)$$

An additional term called stopping function can be added to the speed function in the GAC model [27]. The resulting equation is:

$$\frac{\partial \phi(x,y,t)}{\partial t} = g(f(x,y))(\alpha\kappa(\phi(x,y,t)) + \nu)\left|\nabla\phi(x,y,t)\right| \qquad (8)$$

where $g(f(x, y))$ is the stopping function, which is a positive and decreasing level set function from the gradient of an image $f(x, y)$. This function is written as follows [27]:

$$g(f(x,y)) = \frac{1}{1+\left|\nabla f(x,y)\right|} \qquad (9)$$

According to equation (8), the contours move in the normal direction with a speed $F = g(f(x, y))(\alpha\kappa(\phi(x, y, t)) + \nu)$ and stop on the boundary, where $g$ disappears.

## IV. Experiments and Results

### A. Database

Experiments to evaluate WBC segmentation results are carried out using three publicly available databases:

- *Acute Lymphoblastic Leukemia Image Database for Image Processing (ALL-IDB)* [2]:

  This database was collected by the Department of Information Technology - Università degli Studi di Milano. It contains 265 microscope images which have single cells or individually separated multiple cells in each image. The magnification ranges from 300 to 500. Images were captured using an optical laboratory microscope coupled with a Canon PowerShot G5 camera of 2592×1944 pixels resolution. Images are divided into three sets, depending on the characteristics of the cells they contain:

  *L1:* Cells are small and homogeneous. Nuclei are round shaped and regular.

  *L2:* Cells are large and heterogeneous. Nuclei are irregular and have one or more lobes.

  *L3:* Cells are moderately large in size and homogeneous. They have one or more nuclei. Nuclei are regular and round-oval in shape.

- *Wadsworth Centre* [3]:

  This database contains 150 images of normal blood slides with different features. High resolution and higher magnification ranging from 500 to 1000 was used to get single cell images that have one or more nuclei, and lower magnification was used to get multiple cells in an image. The contrast between the cell and the background depends on the thickness and lightness of the smear, the illumination, and the staining process used to stain the nucleus (Giemsa stain, Wright stain or Wright-Giemsa stain).

- *Berkeley Segmentation Database* [31]:

  This database is used to measure and benchmark the performance of segmentation methods and consists of 300 images of single WBCs that have one or more nuclei. Ground truths of nuclei of WBCs are available for each single cell image that was manually segmented by a number of human subjects.

### B. Proposed Approach

The proposed method of segmentation using level set methods via GACs was implemented using Matlab 2016a. It was tested using 300 digital blood smear images of different WBCs types (150 single and multiple cell images from ALL-IDB and 150 single cell images from the Wadsworth Centre database). It was also tested and benchmarked using the 300 images of the Berkeley Segmentation Database.

The steps of the proposed approach are shown Fig.4. The result of the segmentation process is shown in Figures 5, 6 and 7. Fig.5 shows an original WBC image, including six of the WBC types and the steps of segmentation using level set methods via GACs. Segmented cells nuclei are shown in Fig.6. Fig.7 shows a comparison using level set method via GACs and PACs.

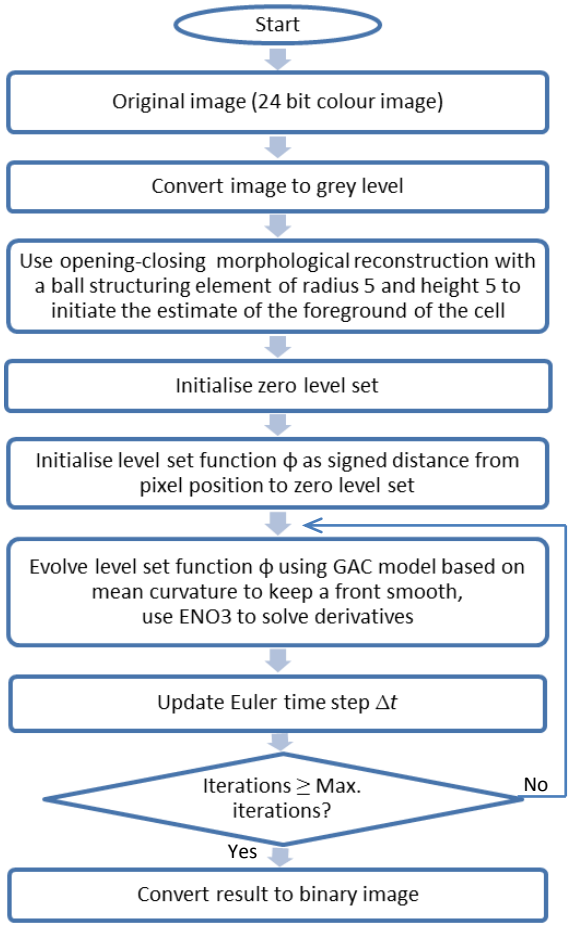


Fig. 4. Flowchart of the proposed method to segment WBCs.

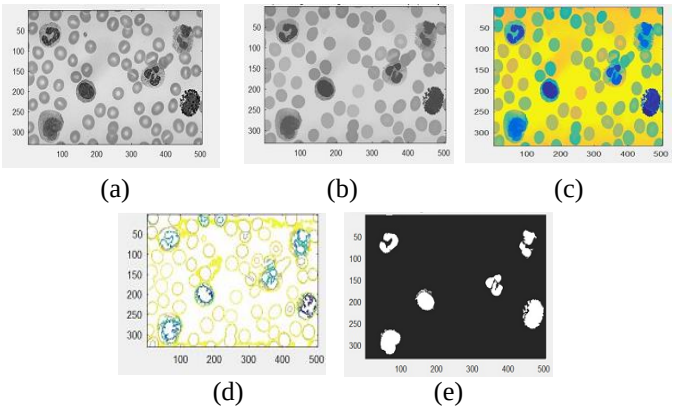


Fig. 5. WBC segmentation using level set methods via GACs. a) WBC image, b) opening–closing reconstruction, c) level set method with normal direction and colour map, d) level set method via GAC using image gradient, and e) segmented nuclei of WBC.

Fig. 6. Cells nuclei from segmented image. Pixel intensity values of 1 (white) and 0 (black) are used for the foreground and background, respectively.


Fig. 7. Band neutrophil segmentation example. a) Band neutrophil cell image, b) cell nucleus segmented using level set method via PACs [32], and c) cell nucleus segmented using level set method via GACs (proposed method).

### *C. Results and Benchmark*

Different segmentation methods are evaluated and compared in this section using five indices: Boundary Displacement Error (BDE), Global Consistency Error (GCE), Variation of Information (VOI), Jaccard Distance error (JD), and Rand Index (RI) [28][29]. These indices provide a measure of how similar a segmented image is to a ground truth that is segmented manually. BDE computes the average displacement between the boundaries resulting of two segmentations; it ranges between $[0,\infty)$ in pixel units, where a lower value is better. GCE measures the extent to which one segmentation is a refinement of the other; it ranges between [0, 1], where lower is better. VOI computes the amount of one result not contained in the other; it ranges between $[0,\infty)$, where higher is better. JD calculates the accuracy of the segmentation; JD = 0 is best. RI measures the likelihood of a pair of pixels being grouped consistently in two segmentations, and ranges between $[0,1]$, where higher is better [30].

Table I lists the values of these performance indices for the proposed segmentation algorithm where each value is an average computed over the performance of 300 WBC images (150 single and multiple cell images from ALL-IDB and 150 single cell images from the Wadsworth Centre database).

Table II is a comparison of the performance indices for the proposed segmentation method with other methods. Average values were computed for the proposed segmentation method using the 300 images in the Berkeley Segmentation Database, and compared with average values provided in the Berkeley Segmentation Database for other methods. To quantify the segmentation results, we use four indices from the Berkeley database [31]: RI, VOI, GCE, and BDE, and in addition we compute JD. The performance of the proposed technique is benchmarked against 10 other algorithms: Normalized cut (Ncut), Mean Shift [33], J-image segmentation (JSEG), Multi-scale Ncut (MNcut), Normalized Tree Partitioning (NTP), Texture and Boundary Encoding-based Segmentation (TBES) [34], Ultrametric Contour Maps (UCM), Superpixels and Multilayer Spectral Segmentation (MLSS), Segmentation by Aggregating (SAS), RB-Wavelet, and SOM [35]. As can be seen in the table, the proposed segmentation method results in better performance than all other techniques for all indices except BDE, where the SAS and MLSS algorithms are marginally better.

TABLE I. AVERAGE PERFORMANCE EVALUATION OF PROPOSED SEGMENTATION METHOD FOR EACH WBC TYPE USING 150 SINGLE AND MULTIPLE CELL IMAGES FROM ALL-IDB [2] AND 150 SINGLE CELL IMAGES FROM THE WADSWORTH CENTRE DATABASE [3]. NOTE THAT LOWER VALUES ARE DESIRABLE FOR THE FIRST THREE COLUMNS, WHEREAS HIGHER VALUES ARE DESIRABLE FOR THE LAST TWO COLUMNS.

| Cell type | JD | BDE | GCE | VOI | RI |
|---|---|---|---|---|---|
| Granulocyte | 0.00334 | 15.01 | 0.0025 | 4.89 | 0.9945 |
| Neutrophil | 0.0009 | 16.86 | 0.0005 | 4.16 | 0.9994 |
| Basephil | 0.00018 | 10.44 | 0.0001 | 4.22 | 0.9996 |
| Eosinophil | 0.0014 | 9.25 | 0.0032 | 3.66 | 0.9976 |
| Monocyte | 0.00027 | 11.25 | 0.0001 | 5.69 | 0.9892 |
| Macrophage | 0.00016 | 11.32 | 0.0032 | 4.27 | 0.9762 |
| Dendritic | 0.0022 | 12.48 | 0.0029 | 4.32 | 0.9996 |
| Lymphocyte | 0.0044 | 12.77 | 0.0042 | 3.84 | 0.9809 |
| B-Lymphocyte | 0.00177 | 14.92 | 0.001 | 4.77 | 0.9605 |
| T-Lymphocyte | 0.0003 | 10.01 | 0.005 | 3.22 | 0.9901 |

TABLE II. COMPARISON OF DIFFERENT WBC SEGMENTATION METHODS. PERFORMANCE INDICES FOR THE PROPOSED METHOD ARE COMPARED WITH THOSE PROVIDED IN THE BERKELEY SEGMENTATION DATABASE [31]. THE BEST RESULT OF EACH COLUMN IS HIGHLIGHTED IN BLUE, AND THOSE CASES IN WHICH THESE RESULTS ARE OUTPERFORMED BY THE PROPOSED METHOD ARE HIGHLIGHTED IN GREEN. NOTE THAT LOWER VALUES ARE DESIRABLE FOR THE FIRST THREE COLUMNS, WHEREAS HIGHER VALUES ARE DESIRABLE FOR THE LAST TWO COLUMNS.

| Methods | JD | BDE | GCE | VOI | RI |
|---|---|---|---|---|---|
| Ncut | 0.385 | 17.15 | 0.223 | 2.906 | 0.724 |
| Mean Shift [33] | 0.407 | 14.41 | 0.189 | 1.973 | 0.796 |
| JSEG | 0.039 | 14.4 | 0.199 | 2.322 | 0.776 |
| MNcut | 0.390 | 15.1 | 0.192 | 3.395 | 0.756 |
| NTP | 0.392 | 16.3 | 0.237 | 2.495 | 0.752 |
| TBES [34] | 0.392 | N/A | N/A | 1.76 | 0.8 |
| UCM | 0.394 | N/A | N/A | 1.68 | 0.81 |
| MLSS | 0.039 | 12.21 | 0.018 | 3.055 | 0.814 |
| SAS | 0.393 | 11.29 | 0.178 | 1.685 | 0.832 |
| RB-Wavelet and SOM | 0.391 | 14.19 | 2.112 | 0.211 | 0.796 |
| Proposed Method ‘ GACs’ | 0.003 | 12.5 | 0.0031 | 4.218 | 0.931 |

It was also found that the segmentation of WBCs nuclei using level set methods via GACs is better than other techniques in a number of ways, apart from the better performance indices. Unlike the proposed technique, those listed in Table II worked with simple boundaries, small regions and non-overlapping cells. They also retained more unimportant detail, and those based on PACs did not track the changing topology of cells or nuclei. They did not segment the nuclei of WBCs accurately as shown in Fig.8 and Fig.9. Furthermore, the proposed method gives better ability to discriminate between WBC sub-types. Fig.8(b) shows that the segmentation using the mean shift method [33] produces four cells, where two of them are not WBCs, and nuclei are not properly segmented. Fig.8(c) shows that the proposed method produces two nuclei which have 2 and 3 lobes, which allows to identify the cells as WBC sub-types. Fig.9(b) shows that the segmentation using the texture and boundary encoding-based method [34] produces two nuclei. This leads to consider the WBC as a lymphocyte, when, in fact, it is a neutrophil cell as shown in Fig.9(c).

(a) (b) (c)

Fig.8. Mature eosinophil segmentation example. a) WBC image, b) cells nuclei segmented using mean shift [33], and c) cells nuclei segmented using the proposed level set method via GACs.

(a) (b) (c)

Fig.9. Neutrophil segmentation example. a) Neutrophil cell image, b) cell nuclei segmented using texture and boundary encoding-based segmentation [34], and c) cell nuclei segmented using the proposed level set method via GACs.

The changes in curve topology and boundary gaps of WBCs that MNcut, MLSS, Ncut, mean shift and TBES cannot solve (as shown in Fig.8 and Fig.9), are correctly solved by level set methods via GACs because they preserve the perceptual edge property of active contours. Fig.7 shows an example in which level set method via GACs was applied to an image containing a WBC that has both concavities and boundary gaps. The final result shows the ability of the level set method via GAC to get better boundaries reliably in spite of both gaps and nucleus boundary concavities by contrast with other methods.

The proposed level set method via GACs was tested using a processor Intel(R) Core(TM) i7-4600U CPU 2.70 GHz and MATLAB 2016a. It takes 0.64 seconds to segment one cell and 1.71 seconds to segment one image. Other methods provided in Berkeley Segmentation are as follows: SAS [35] takes 6.44 seconds to segment an image of size 481×321, JSEG takes 4.11 seconds, and mean shift takes 10.4 seconds [33]. By contrast, MNcut, MLSS, Ncut, and TBES [34] take more than 30, 40, 150, and 500 seconds, respectively. All experiments were implemented using MATLAB. According to these results, the level set method via GACs is significantly faster than other methods which use larger time steps to speed up the curve evolution while GACs maintain the stable evolution of the level set function.

## V. CONCLUSION

In this paper, the combination of level set methods and geometrical active contours instead of parametric active contours has been proposed for segmentation of WBCs nuclei. The proposed method has been demonstrated to be very versatile. Since contours can follow intricate details, complex

shapes can be properly extracted. The algorithm has been tested with nuclei images at different stages of maturity and with varying illumination and orientation, without any knowledge of the target shape. The results obtained are satisfactory despite such variations. The performance of the proposed algorithm has been measured and compared with that of other methods using the indices RI, GCE, VOI, JD and BDE. The proposed algorithm yields better segmentation results according to these metrics in all cases, except for boundary displacement error cases where the SAS and MLSS algorithms are marginally better. Further investigation will include feature extraction from the segments and classification of WBCs.

## ACKNOWLEDGMENT

This research was supported/partially supported by Iraqi Higher Education and Scientific Research and Queensland University of Technology. The authors are thankful to Department of Information Technology - Università degli Studi di Milano, Wadsworth Center and Berkeley, who provided the databases, and to pathologist Lubna AL-Sabaawi who provided information about WBCs. The authors are also grateful to Baris Sumengen, whose code has been adapted to create the proposed implementation.

## REFERENCES

[1] M. S. Blumenreich, "The white blood cell and differential count," Clinical Methods: The History, Physical, and Laboratory Examinations, 3rd ed. Boston: Butterworths, 1990.

[2] ALL-IDB "Acute Lymphoblastic Leukemia Image Database for Image Processing," Department of Information Technology - Università degli Studi di Milano, 2005. Available: http://crema.di.unimi.it/~fscotti/all/

[3] Wadsworth Center, New York State Department of Health. Available: http://www.wadsworth.org/

[4] J. Kemal, Laboratory Manual and Review on Clinical Pathology, 2014.

[5] V. L. Clark and J. A. Kruse, "Clinical methods: the history, physical, and laboratory examinations," JAMA, vol. 264, pp. 2808-2809, 1990.

[6] S. Standring, Gray's anatomy: the anatomical basis of clinical practice: Elsevier Health Sciences, 2015.

[7] I. Van Brussel, D. M. Schrijvers, G. R. De Meyer, H. Bult, and W. Martinet, "Dendritic Cells in Atherogenesis: From Immune Shapers to Therapeutic Targets," INTECH Open Access Publisher, 2013.

[8] P. E. Norgren, A. V. Kulkarni, and M. D. Graham, "Leukocyte image analysis in the diff3 system," Pattern Recognition, vol. 13, pp. 299-314, 1981.

[9] B. R. Kumar, D. K. Joseph, and T. Sreenivas, "Teager energy based blood cell segmentation," International Conference on Digital Signal Processing, pp. 619-622, 2002.

[10] G. Dong, N. Ray, and S.T. Acton, "Intravital leukocyte detection using the gradient inverse coefficient of variation", IEEE Transactions on Medical Imaging, vol. 24, no. 7, pp. 910-924, 2005.

[11] O. Sarrafzadeh and A. M. Dehnavi, "Nucleus and cytoplasm segmentation in microscopic images using K-means clustering and region growing," Advanced Biomedical Research, vol. 4, p. 174, 2015.

[12] Osher and R. Fedkiw, Level set methods and dynamic implicit surfaces, vol. 153: Springer Science & Business Media, 2006.

[13] T. McInerney and D. Terzopoulos, "Deformable models in medical image analysis: a survey," Medical Image Analysis, vol. 1, pp. 91-108, 1996.

[14] C. Xu, A. Yezzi Jr, and J. L. Prince, "On the relationship between parametric and geometric active contours," Conference on Signals, Systems and Computers, pp. 483-489, 2000.

[15] C. Xu, A. Yezzi Jr, and J. L. Prince, "A summary of geometric level-set analogues for a general class of parametric active contour and surface models," IEEE Workshop on Variational and Level Set Methods in Computer Vision, pp. 104-111, 2001.

[16] H. Tirandaz, S. Azadi, and M. Sharifi, "A New Approach for Parametric Active Contour Segmentation," World Applied Sciences Journal, vol. 28, pp. 2010-2015, 2013.

[17] V. Caselles, F. Catte, T. Coll, and F. Dibos, "A Geometric Model for Active Contours in Image Processing," Numerische Mathematik, vol. 66, pp. 1-31, 1993.

[18] K. Museth, D. E. Breen, R. T. Whitaker, and A. H. Barr, "Level set surface editing operators," ACM Transactions on Graphics, vol. 21, pp. 330-338, 2002.

[19] F. Precioso, "Contours actifs paramétriques pour la segmentation d'images et vidéos," Université Nice Sophia Antipolis, 2004.

[20] C. Li, "Active Contours, Level Sets, and Image Segmentation," Institute of Imaging Science, Vanderbilt University. Available: http://www.vuiis.vanderbilt.edu/~licm.

[21] W. Yu, H. K. Lee, S. Hariharan, W. Bu, and S. Ahmed, "Level set segmentation of cellular images based on topological dependence," Advances in Visual Computing, Springer, pp. 540-551, 2008.

[22] Q. Wenhua, W. Liang, and Q. Zhenzhen, "White Blood Cell Nucleus Segmentation Based on Canny Level Set," Sensors & Transducers, vol. 180, p. 85, 2014.

[23] K. Chinnathambi, A. Ramasamy, and P. Ramachandran, "Robust segmentation of cancer affected white blood cells using modified level set algorithm," International Journal of Simulation: Systems, Science and Technology, vol. 14, 2014.

[24] N. H. Salman, "Level Set Methods Implementation for Image Levelsets and Image Contour," IJCSNS, vol. 9, p. 199, 2009.

[25] T. F. Chen, "Medical image segmentation using level sets," Technical Report. Canada, University of Waterloo, pp.1-8, 2008.

[26] A. Yezzi Jr, S. Kichenassamy, A. Kumar, P. Olver, and A. Tannenbaum, "A geometric snake model for segmentation of medical imagery," IEEE Transactions on Medical Imaging, vol. 16, pp. 199- 209, 1997.

[27] M. Airouche, L. Bentabet, and M. Zelmat, "Image segmentation using active contour model and level set method applied to detect oil spills," in World Congress on Engineering, pp. 1-3, 2009.

[28] R. C. Gonzalez, Digital image processing: Pearson Education India, 2009.

[29] G. L.-E. W. Yong, "Evaluation measures for segmentation," matrix, vol. 1, p. 2.

[30] C. Solomon and T. Breckon, Fundamentals of Digital Image Processing: A practical approach with examples in Matlab: John Wiley Sons, 2011.

[31] http://www.eecs.berkeley.edu/Research/Projects/CS/vision/groupin

[32] J.-F. Ma, K. Hou, S.-L. Bao, and C. Chen, "A new level set model for cell image segmentation," Chinese Physics B, vol. 20, p. 028701, 2011.

[33] Z. Liu, J. Liu, X. Xiao, H. Yuan, X. Li, J. Chang, et al., "Segmentation of White Blood Cells through Nucleus Mark Watershed Operations and Mean Shift Clustering," Sensors, vol. 15, p. 22561, 2015.

[34] Y.-K. Chan, M.-H. Tsai, D.-C. Huang, Z.-H. Zheng, and K.-D. Hung,"Leukocyte nucleus segmentation and nucleus lobe counting," BMC Bioinformatics, vol. 11, p. 558, 2010.

[35] Z. Li, X.-M. Wu, and S.-F. Chang, "Segmentation using superpixels: A bipartite graph partitioning approach," IEEE Conference on Computer Vision and Pattern Recognition, pp. 789-796. 2012.